Ab Initio Monte Carlo Simulated Annealing Study of $HCl(H_2O)_n$ ($n = 3, 4$) Clusters

Daniel E. Bacelo, R. C. Binning, Jr., and Yasuyuki Ishikawa*

Department of Chemistry, University of Puerto Rico, P.O. Box 23346, San Juan, PR 00931-3346

Received: October 30, 1998; In Final Form: April 20, 1999

Low-lying structures of HCl $(H_2O)_n$ ($n = 3, 4$) clusters have been studied by ab initio Monte Carlo simulated annealing (MCSA), a procedure which efficiently samples minima on a potential energy surface. In the Monte Carlo simulated annealing procedure, energies were computed ab initio at each Monte Carlo step by the B3-LYP density functional method with 6-31G* basis sets. All geometries of the isomers found for each cluster were refined in full conventional geometry optimizations, and frequency analyses were performed at both the B3-LYP and MP2 levels with 6-311+G** basis sets. The stability of the B3-LYP and MP2 energy orderings was tested in single point QCISD(T) calculations performed at the MP2 optimized geometries. Only isomers with strong H−Cl interaction were found for $HCl(H_2O)_3$. However, both associated- and dissociated-HCl structures of $HCl(H_2O)_4$ were found.

1. Introduction

In the past decade the study of small $HCl-H_2O$ clusters has been an active area of research, for its intrinsic interest and for the role such clusters play in the ozone depletion cycle. Heterogeneous reactions of chlorine compounds on polar stratospheric cloud (PSC) particles are important in the destruction of ozone in the antarctic and the arctic.[1−5] On ice surfaces the fairly inert species $ClONO_2$ and HCl are converted to Cl_2 and HOCl, which are in turn photolyzed to chlorine atoms that induce ozone-destroying chain reactions.[6] Experiments[7] have shown ionization and solvation to be fundamental to the mechanism by which chlorine is activated on PSCs. The reactions are slow in the gas phase but catalyzed by ice surfaces.[8] As it has come to be recognized that thin layers of mobile water molecules are likely to be present on PSCs, even at very low temperatures, due to daytime radiation, mechanisms by which chlorine-containing compounds react with small numbers of water molecules to produce active species have gained favor.[9]

Amid the proliferation of experimental studies there is still a paucity of detailed structural and energetic information about the species formed when HCl and water interact in small clusters. Delzeit et al.[10] have studied the infrared spectrum of HCl and water adsorbed on ice. Their results show coincidences in the stretching frequencies observed in HCl adsorbed on ice and in the $H_3O^+Cl^-$ complex which indicate that it is difficult to distinguish the associated from the ionized form. Theoretical electronic structure and optimization methods can potentially contribute to the identification and characterization of the variety of forms to be expected in small HCl−water clusters. Thus we have undertaken to study the clusters of HCl with three and four water molecules with the aim of identifying as many low-lying structures as possible and of determining their relative energies.

There have been several theoretical studies of HCl interacting with liquid water and with ice which indicate that the transition in cluster size from three to four waters is significant to the problem of determining the conditions necessary for HCl to ionize. In a classical trajectory study of the adherence of HCl to ice, Kroes and Clary[11] found only nondissociated adsorbed species. In a subsequent molecular dynamics (MD) simulation of HCl on an ice surface at 190 K, Robertson and Clary[12] found that dissociation of HCl is energetically feasible and raised a question as to the minimum number of water molecules needed to solvate an ionized HCl. An MD study by Gertner and Hynes[13] also found ionized HCl on the simulated surface of stratospheric ice particles. Recently, Packer and Clary[14] have studied HCl clustered with as many as three waters, at the Møller−Plesset second-order perturbation theory (MP2)[15] level, and found only a nondissociated stable structure in which HCl is hydrogen bonded to a cyclic three-water cluster. They inferred that in the gas phase HCl will not dissociate to ions in complexes of fewer than four waters. The experimental study of Amirand and Maillard[16] of $(HCl)_m(H_2O)_n$ clusters below 50 K also determined that four waters were required to dissociate an HCl. It appears then that the transition from three- to four-water clusters corresponds to the transition to stability of dissociated HCl.

$HCl(H_2O)_4$ has also been investigated by Planas et al.[17] who, in a theoretical study of proton transfer by acids in aqueous solution, reported an ionic structure as the only minimum on the potential energy surface of $HCl(H_2O)_4$. Geiger and co-workers[18] have reported an ab initio calculation of the binding energy of HCl to water tetramer, mimicking adsorption on the 0001 surface of hexagonal ice. The mechanism of HCl ionization in water was studied by Ando and Hynes[19] in Monte Carlo (MC) simulations. They characterized the ionization as a complex set of adiabatic, nontunneling proton-transfer processes.

Our aim in studying $HCl(H_2O)_n$ ($n = 3, 4$) clusters is to identify as many stable configurations as possible, including all of the metastable clusters lying near in energy to the global minimum. The difficulty of identifying all low lying minima on a cluster potential surface increases rapidly with cluster size. The combination of chemical intuition with conventional optimization methods, which is effective in identifying the configurational isomers of small clusters, is rapidly overmatched as size increases. Thorough examination of the potential surfaces of medium- to large-sized clusters requires an efficient sampling method, such as Monte Carlo Simulated Annealing (MCSA).[20]

* To whom correspondence should be addressed: e-mail, ishikawa@rrpac.upr.clu.edu; fax, (787) 751−0625.

10.1021/jp9843003 CCC: $18.00
Published on Web 05/29/1999

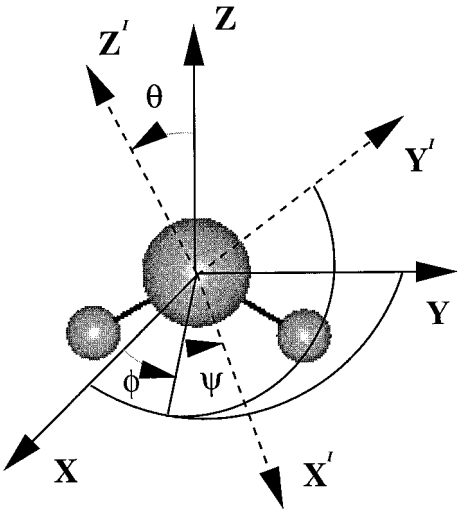

Figure 1. Water molecule, original and rotated Cartesian coordinates, and Euler angles characteristic of a molecular rotation.

MCSA is based on the Metropolis algorithm,[21] which has been shown to be effective in locating minima on complicated energy hypersurfaces.[22] We employ ab initio MCSA;[23,24] energies at each MC step are calculated ab initio, rather than with an analytic potential function previously fit to the surface. When a minimum structure is identified, it is refined by conventional gradient search optimization. The energy ordering is established accurately in single-point calculations at the MP2 minimum energy structures with progressively higher-order ab initio methods.

2. Methods

Ab initio MCSA is a traditional Metropolis Monte Carlo procedure modified in two ways.[23,24] Energies are computed by ab initio electronic structure methods rather than via analytic function, and the temperature of the MC simulation is not held constant, but gradually lowered to anneal the system. An MCSA procedure is started at a given temperature by calculating the total energy of an initial cluster configuration $\{R_0\}$. A complication in MC simulation of HCl−water clusters is that the procedure must describe aggregations in which HCl is both ionized and bound. For this reason the motions of the H and Cl of HCl are treated independently. In addition, one water molecule is selected at random to be moved atom-by-atom, allowing the simulation of the formation of hydronium ion. For molecules moved atom-by-atom the atomic Cartesian coordinates are displaced by a random fraction of a preselected stepsize, ΔR,

$$x_{\text{new}} = (x_{\text{old}})(\zeta_x - 0.5)(\Delta R) \tag{1}$$

Equation 1 is applied to each of the Cartesian coordinates of the atom; ζ is a different random number on [0.0,1.0] for each coordinate. The maximum displacement parameter (ΔR) is adjusted to give a global step acceptance ratio of between 0.1 and 0.5. The remaining molecules in each MC step are treated as units, randomly translated and rotated in three-dimensions. The angular stepsize, ΔA, is chosen by a criterion similar to that applied to ΔR. Figure 1 illustrates the Euler angles of the body-fixed rotation. This partitioning into atomic and molecular motions is less time consuming than complete atom-by-atom treatment but has the flexibility to sample the important configurations.

After each movement of an atom or molecule, the energy of the newly created configuration is evaluated and the change in the total energy of the cluster,

$$\Delta E = E\{R_{\text{new}}\} - E\{R_{\text{old}}\} \tag{2}$$

is computed. If ΔE is negative, the new configuration, $\{R_{\text{new}}\}$, is accepted as $\{R_{\text{old}}\}$ for the next random move. If ΔE is positive, the new configuration is accepted with a probability given by the Boltzmann factor,

$$p = \exp(-\Delta E / kT) \tag{3}$$

The Metropolis acceptance criterion permits both uphill and downhill movement on the potential energy surface, the magnitude of said motions determined by the temperature. MCSA can, therefore, avoid being trapped in local minima. For a given temperature, a number of Metropolis samplings are performed to simulate structural equilibria.

After a complete cycle in which every atom is moved, an annealing adjustment is made. The next cycle proceeds with a new lower temperature,

$$T_{\text{new}} = \gamma T_{\text{old}} \tag{4}$$

where γ is termed the quenching factor. In this study values of γ ranged from 0.950 to 0.999. Simulated annealing is conceptually based on the crystal forming process. During the simulation the temperature is lowered slowly from a sufficiently high temperature to a "freezing" temperature via the temperature-quenching scheme of Kirkpatrick and co-workers.[20,22] The choice of quenching factor affects the outcome of a simulation. Slow enough annealing locates the global minimum on the Born−Oppenheimer surface, while faster annealing can find local minima. Stepsizes ΔR and ΔA are correspondingly lowered to maintain detailed balance, e.g.,

$$\Delta R_{\text{new}} = \gamma \Delta R_{\text{old}} \tag{5}$$

In our MCSA procedure, energies are computed ab initio at each Monte Carlo step using density functional theory (DFT) with Becke's three parameter hybrid plus the Lee, Yang, and Parr correlation functional (B3-LYP)[25,26] and 6-31G* basis sets.[27] DFT methods offer savings in computational time over the conventional MP2 method which has been applied successfully in studies of metal and molecular clusters.[23,24] Recent progress in developing nonlocal corrections to the local density approximation[28−31] has produced DFT methods which reliably predict geometries of hydrogen bonded systems.[32,33]

The electronic structure calculations were performed with the GAUSSIAN 94[34] suite of programs. Structures obtained by simulated annealing were checked and refined by standard geometry optimization at the B3-LYP and MP2 levels of theory. The basis sets were progressively improved by adding diffusion and polarization functions. For each optimization, frequency calculations were performed to confirm that the structures were true minima at each theoretical level. A final energy ordering of the various minima was established in single-point quadratic singles and doubles configuration interaction plus perturbative triples (QCISD(T))[35] calculations at the MP2 optimized structures with 6-311+G** basis sets for $HCl(H_2O)_3$ and 6-311+G* for $HCl(H_2O)_4$. HCl, H_2O, and $(H_2O)_4$ were also optimized at the MP2 and B3-LYP levels with 6-311+G** basis sets to permit the energetics of cluster formation to be examined.

3. Results and Discussion

A number of DFT−MCSA simulations of each cluster were performed with different starting geometries. The initial tem-

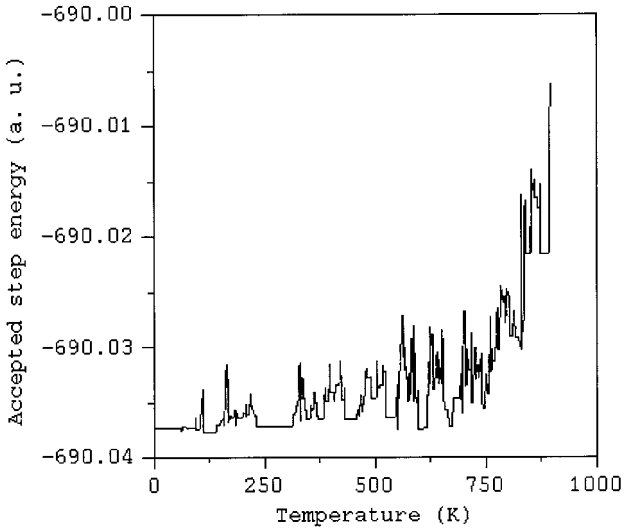

Figure 2. Plot of the energies of accepted Monte Carlo steps versus temperature in a simulated annealing procedure for $HCl(H_2O)_3$.

peratures used in each simulation lay in the range of 600−1000 K, with quenching factors of from 0.950 to 0.999. The procedure by which initial conditions are chosen has been discussed more fully in refs 20 and 23. Figure 2 illustrates the ranges of cluster energies encountered in a typical simulation. The variation in total energy of an $HCl(H_2O)_3$ cluster obtained at each accepted step at a given temperature is plotted versus temperature. In a number of instances, the energy is seen to rise, behavior permitted by the Metropolis algorithm.

DFT−MCSA simulations of $HCl(H_2O)_3$ produced twelve geometries. Conventional B3-LYP and MP2 optimizations with 6-311+G** basis sets reduced the number of distinct structural minima to five. MP2 optimized structures of the five isomers are shown in Figure 3. Four of the simulations terminated with isomer A1, confirming it as the global minimum with a confidence ratio[22] well over 99%. A2 of Figure 3 is a local minimum cluster structure derived from A1 by "flipping", or turning through an angle of approximately 180°, one or more of the free hydrogens. A set of such "torsional isomers" may be generated from each of the minimized structures,[36−38] but we have restricted the number presented to one pair from each class of cluster we have examined. We hope thereby to provide an adequate idea of the structural and energetic variations to be expected in these species without obscuring discussion of the structural isomers that are the primary interest of this study. Geometrical parameters for the three-water clusters appear in Tables 1 and 2. All isomers show strong H−Cl interaction, with interatomic distances of 1.27−1.39 Å, quite near the equilibrium bond length of gas-phase HCl. The predicted equilibrium bond length of isolated HCl with 6-311+G** basis sets is 1.287 Å at the B3-LYP and 1.273 Å at the MP2 level.

For $HCl(H_2O)_4$, five isomers were found. Three of these show little perturbation of the HCl bond, while two display either significant elongation of the bond or actual dissociation. Figures 4 and 5 exhibit the MP2 structures of the $HCl(H_2O)_4$ isomers. The structures of Figure 4 are those in which HCl is undissociated, while Figure 5 shows the structures in which dissociation has taken place. Each figure shows one pair of torsional isomers. Selected geometrical parameters are tabulated in Tables 3 and 4 for the isomers displayed in Figures 4 and 5, respectively, and data for the torsional isomers are included. While we are confident that our investigation has revealed all, or nearly all,

TABLE 1: Selected Geometrical Parameters of Optimized Structures of $HCl(H_2O)_3$[a]

	A1		A2		B	
parameter	B3-LYP	MP2	B3-LYP	MP2	B3-LYP	MP2
Cl−H(1)	1.358	1.316	1.356	1.313	1.315	1.296
H(1)−O(1)	1.585	1.676	1.594	1.684	1.804	1.806
O(1)−H(2)	0.988	0.979	0.986	0.977	0.985	0.977
O(1)−H(3)	0.962	0.960	0.962	0.960	0.963	0.960
H(2)−O(2)	1.726	1.764	1.747	1.785	1.781	1.803
O(2)−H(4)	0.981	0.974	0.981	0.974	0.975	0.972
H(4)−O(3)	1.790	1.816	1.791	1.817	1.896	1.906
O(3)−H(5)	0.972	0.966	0.972	0.966	0.970	0.964
H(5)−Cl	2.370	2.392	2.370	2.393	4.272	3.243
Cl−H(1)−O(1)	174.572	173.318	174.670	172.994	180.407	167.873
Cl−H(5)−O(3)	159.530	159.588	159.797	159.913	133.220	100.711
O(2)−H(4)−O(3)	166.660	166.201	167.090	166.906	145.050	144.882
H(2)−O(1)−H(3)	107.071	105.150	107.268	105.572	107.213	105.861

[a] Distances in angstroms, angles in degrees. All optimizations were performed with 6-311+G** basis sets. Parenthetic numbering of atoms corresponds to Figure 3.

TABLE 2: Selected Geometrical Parameters of Optimized Structures of $HCl(H_2O)_3$[a]

	C		D		E	
parameter	B3-LYP	MP2	B3-LYP	MP2	B3-LYP	MP2
Cl−H(1)	1.3893	1.3318	1.3640	1.3189	1.2911	1.2747
H(1)−O(1)	1.4991	1.6149	1.5711	1.6662	5.0688	4.7727
O(1)−H(2)	0.9756	0.9683	0.9749	0.9690	0.9837	0.9704
O(1)−H(3)	0.9756	0.9683	0.9740	0.9678	2.8110	2.8522
H(2)−O(2)	1.8989	1.9680	1.8508	1.8793	1.8903	1.9357
H(3)−O(3)	1.8979	1.9679	1.9250	1.9745	1.8905	1.9349
O(3)−H(4)	0.9662	0.9627	0.9677	0.9636	0.9838	0.9704
H(4)−Cl	2.8866	2.8573	2.6809	2.6759	3.7081	3.5975
Cl−H(1)−O(1)	170.1063	168.9113	169.7802	168.6409	18.48	19.65
O(2)−H(2)−O(1)	149.3421	144.4684	174.5989	174.9796	148.0509	147.219
H(2)−O(1)−H(3)	107.2108	105.2032	107.6831	105.7233	21.28	41.76

[a] Distances in angstroms, angles in degrees. All optimizations were performed with 6-311+G** basis sets. Parenthetic atomic numbering corresponds to Figure 1.

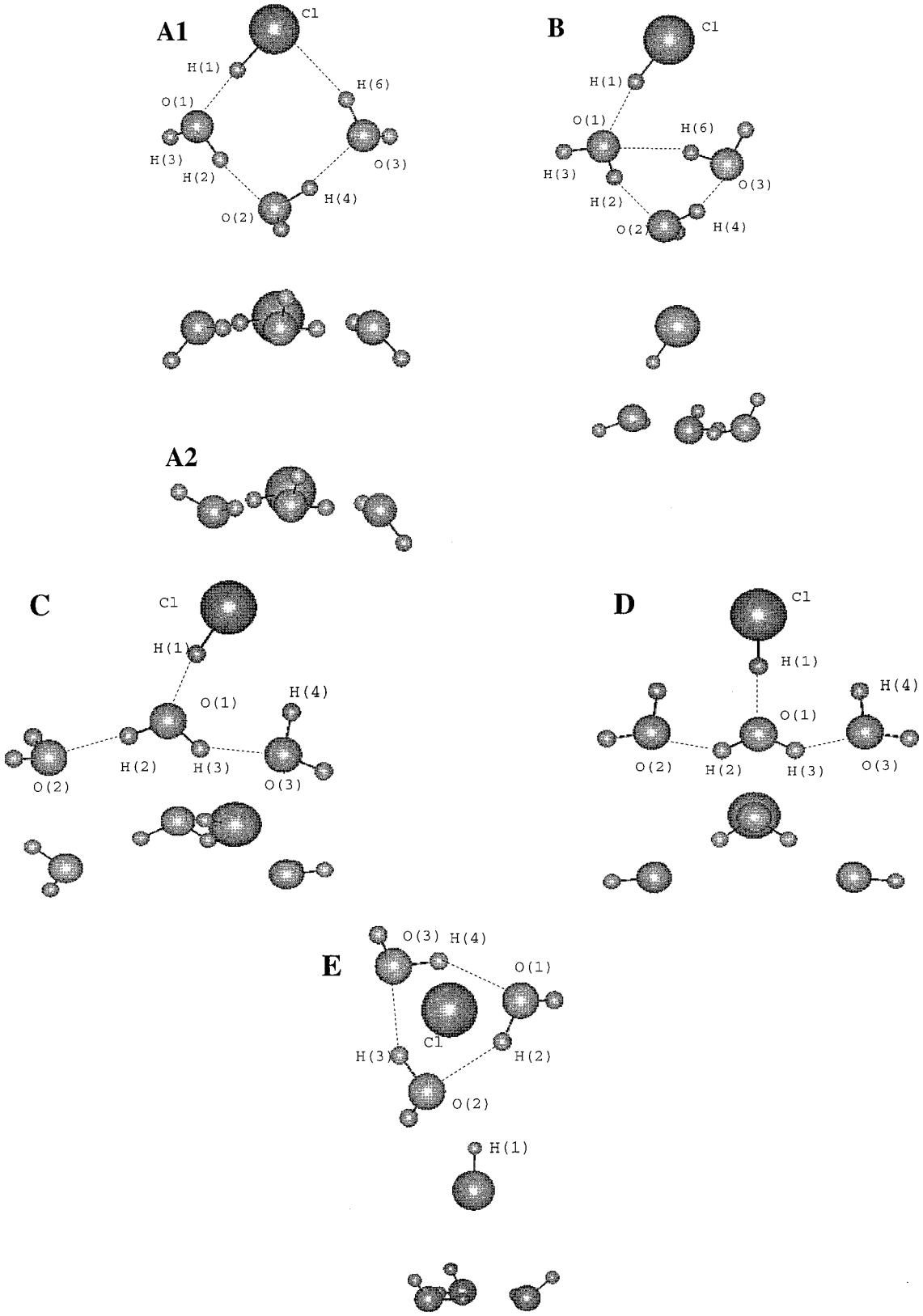

Figure 3. Structural isomers of $HCl(H_2O)_3$, top and side views. A2, torsional isomer of A1, is shown in side view only; compare the positions of the free hydrogens above and below the plane formed by the oxygen atoms to those in A1.

of the low-lying isomers of $HCl(H_2O)_3$, the complexity of the four-water surface makes it likely that we have not found all possible structures for this cluster. Still, we are confident in having located the global minimum structure. This is the structure that emerges from a sequence of simulations in the limit as the quenching factor approaches unity.

Some B3LYP minima proved to be spurious. Several authors[32,39,40] have found that DFT optimization of hydrogen-bonded systems can locate more structures than does MP2 and that some of the minima are therefore spurious. We[32] have noted instances in which DFT methods have underestimated the strengths of hydrogen bonds, producing nonphysical open

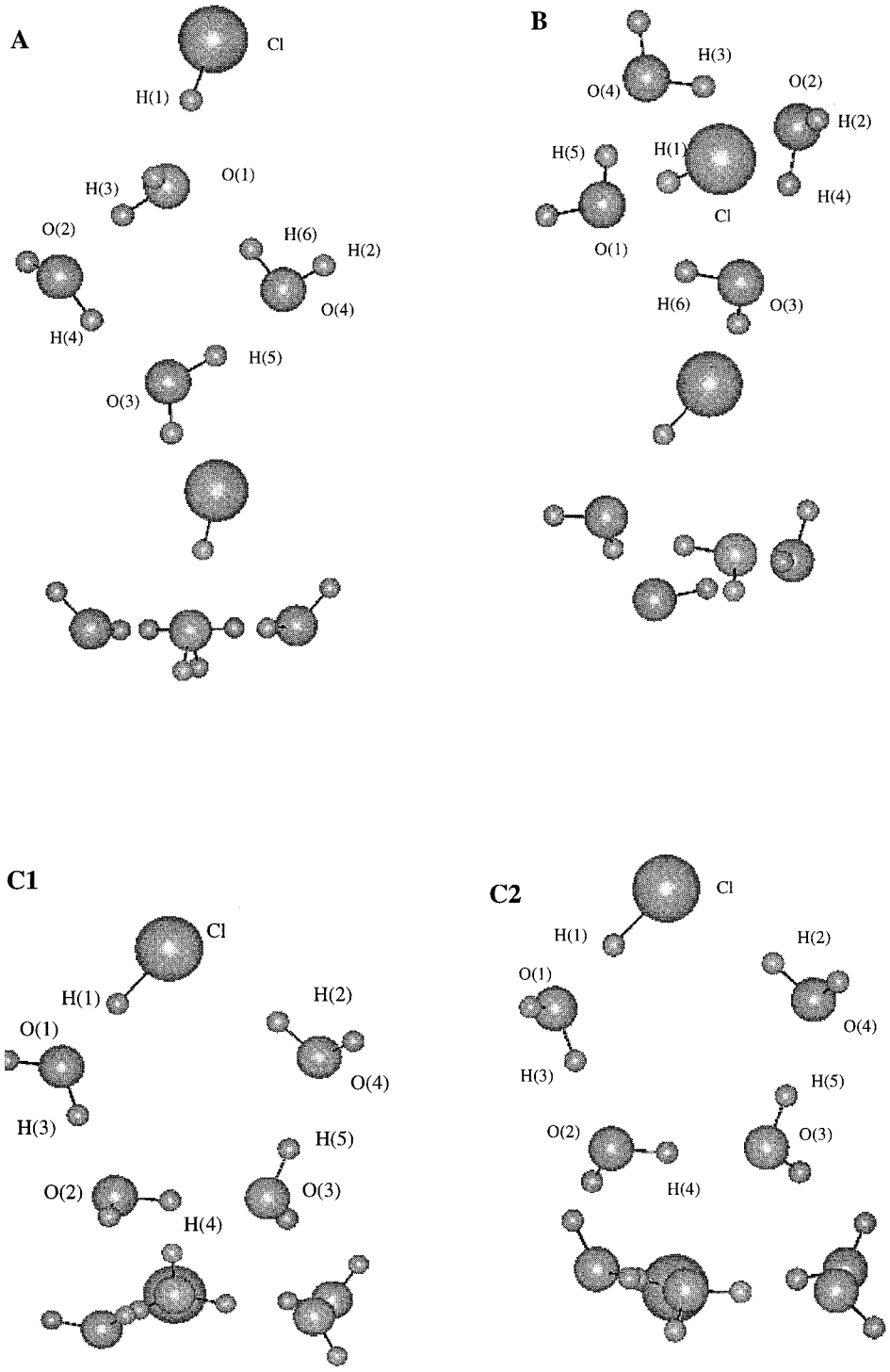

Figure 4. Isomers of $HCl(H_2O)_4$ in which HCl is undissociated, top and side views. C1 and C2 are torsional isomers.

structures as minima. In recent work on hydrated clusters of HCl, Re et al.[39] have reported B3LYP three- and four-water structures that are not minima at the MP2 level. Smith et al.[40] have reoptimized, at the MP2 level with the original D95++-(p,d) basis sets, one of the three-water cluster structures reported by Re et al. (ref 39, Figure 1, structure IIIb), beginning at the original B3LYP geometry. They found a structure in which HCl remains undissociated, in contrast to the dissociated structure obtained at the B3LYP level. We have repeated the exercise with one of the four-water structures reported by Re et al. (ref 39, Figure 2, structure IVd). At the MP2 level the reported structure is not a minimum, and upon optimization merges into another of the reported structures (ref 39, Figure 2, structure IVb; this work Figure 5, structure E).

Although DFT potential surfaces of hydrogen bonded systems can be somewhat more convoluted than MP2, this and other studies have not found the aberrations to be dramatic, and so among the DFT minima are minima near those to be found by MP2 optimization. In this sense, and provided the DFT structures are reoptimized at the MP2 level, DFT optimizations of these systems are reliable. The fact that each DFT minimum energy structure must be confirmed by conventional MP2 optimization encumbers the process of searching the potential surface. Still the speed with which the DFT−MCSA method

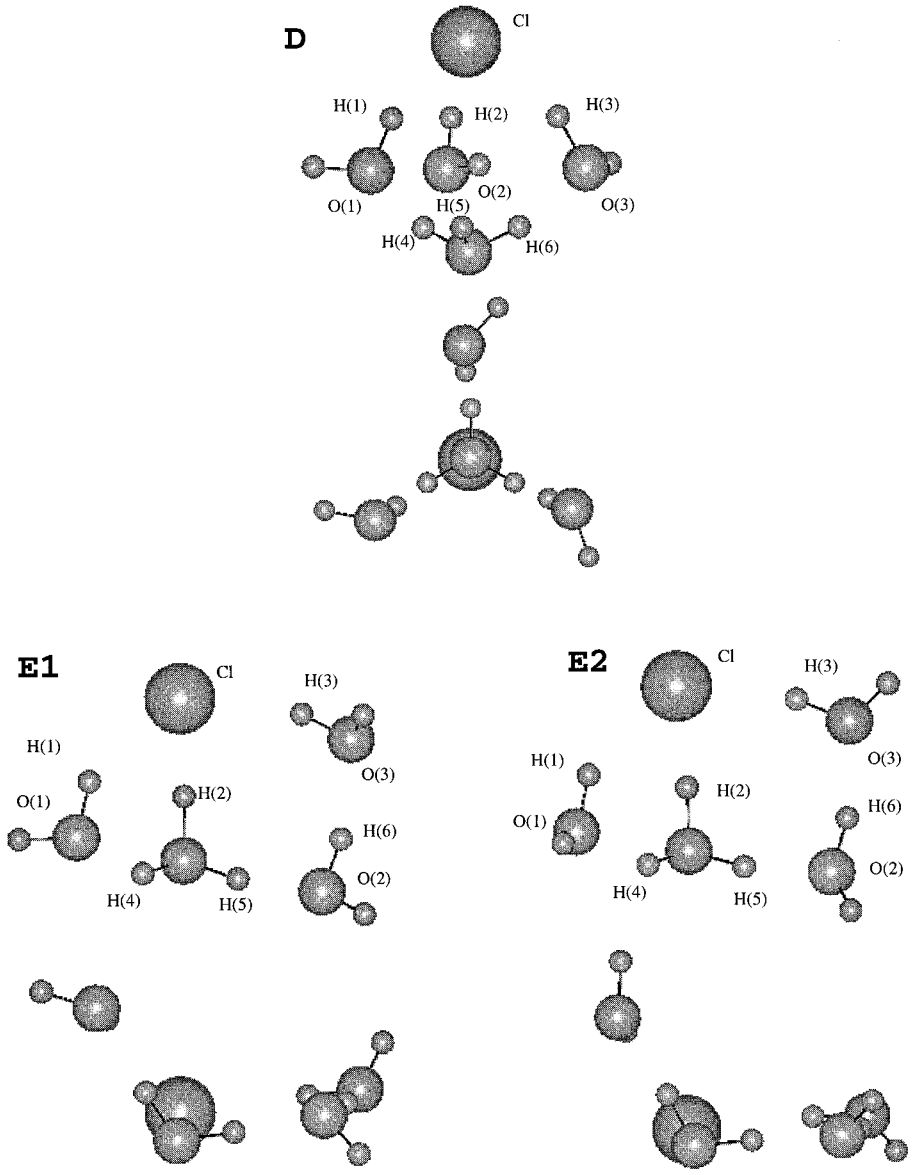

Figure 5. Isomers of $HCl(H_2O)_4$ in which HCl is dissociated, top and side views. E1 and E2 are torsional isomers.

TABLE 3: Selected Calculated B3-LYP/6-311+G and MP2/6-311+G** Interatomic Distances of $HCl(H_2O)_4$ Isomers in which H and Cl are Bonded**[a]

	isomer A		isomer B		isomer C1		isomer C2	
distances	B3-LYP	MP2	B3-LYP	MP2	B3-LYP	MP2	B3-LYP	MP2
Cl−H(1)	1.316	1.293	1.336	1.292	1.367	1.319	1.372	1.323
Cl−H(2)	4.403	3.065	2.564	2.948	2.318	2.350	2.301	2.314
H(1)−O(1)	1.797	1.834	1.677	1.875	1.541	1.641	1.533	1.632
H(3)−O(2)	1.687	1.711	1.721	1.764	1.694	1.728	1.683	1.721
H(4)−O(3)	1.752	1.766	1.980	1.838	1.730	1.753	1.747	1.773
H(5)−O(4)	1.790	1.797	1.792	1.725	1.770	1.792	1.766	1.788
H(6)−O(1)	1.874	1.930	4.486	1.913				

[a] Distances are in angstroms. Atomic identification numbers correspond to those in Figure 4.

samples the surface outweighs the additional time required to confirm the structures that are located, and the advantage increases with the size of the system.

3.1. Optimized Geometries of $HCl(H_2O)_3$. The most stable structure of the three-water cluster is a nearly planar cyclic quadrilateral with the chlorine and oxygens at the corners (isomer A1, Figure 3). Each H_2O acts as both a single hydrogen bond donor and a single acceptor. The free hydrogens of the water molecules lie alternately above and below the buckled plane. The elongation of the H−Cl bond (1.358 Å at the B3-LYP and 1.316 Å at the MP2 levels) indicates strong participation of the molecule in the ring. HCl acts as the donor to a strong hydrogen bond, while one water interacts weakly with chlorine. Isomer A1 has been reported by Packer and Clary.[14] Because they employed basis sets comparable in quality to those used in this study, their reported geometry is essentially identical to ours. Small water clusters have been intensely theoretically studied;[41−43] A1 is similar to the structure found to be most stable for isolated water tetramer in experimental and theoretical studies, but with HCl replacing a water. The distortion of the

TABLE 4: Selected Interatomic Distances in $HCl(H_2O)_4$ Clusters in which H−Cl is Dissociated, Determined in B3-LYP and MP2 Optimizations with 6-311+G Basis Sets[a]**

	isomer D		isomer E1		isomer E2	
distances	B3-LYP	MP2	B3-LYP	MP2	B3-LYP	MP2
Cl−H(1)	2.104	2.069	2.364	2.398	2.378	2.393
Cl−H(2)	2.106	2.069	1.804	1.706	1.788	1.704
Cl−H(3)	2.103	2.069	2.186	2.174	2.176	2.171
O(1)−H(4)	1.544	1.534	1.714	1.750	1.726	1.743
O(2)−H(5)	1.545	1.534	1.528	1.547	1.551	1.561
O(3)−H(6)	1.544	1.534	1.689	1.709	1.691	1.710

[a] Distances are in angstroms. Atomic identification numbers correspond to those in Figure 5.

cyclic structure caused by HCl is reflected in the hydrogen bond lengths. The optimum structure of $(H_2O)_4$ has a mean H-bond distance of 1.775 Å at the B3-LYP and 1.789 Å at the MP2 levels, with small deviations from the mean. Note the relatively wide range of hydrogen bond lengths in isomer A1, presented in Table 1. The data in Tables 1 and 2 show that in general the B3-LYP HCl bond lengths are underestimated in comparison with the MP2, while hydrogen bond distances are overestimated.

Mulliken gross atomic charges can be used to gauge the extent of charge transfer among species. The charges on HCl in isomer A1 are H (0.35) and Cl (−0.35), while in isolated HCl they are about half that, H (0.163) and Cl (−0.163), a magnitude of charge migration which is consistent with hydrogen-bond formation. Charges for H_2O in the same basis sets are H (0.26) and O (−0.51). In $(H_2O)_4$ oxygens carry charges of −0.72 au, H-bond hydrogens 0.44 au, and free hydrogens 0.28 au. The acceptor oxygen atom in the HCl H bond of isomer A1, O(1), is more negative (−0.71) than is an oxygen in free water. Non-hydrogen-bond hydrogens retain the charges they display in free water. The charges on O(3) and H(5) indicate that the interaction between H(5) and Cl is too weak to be considered a hydrogen bond.

A2 is a torsional conformer of $HCl(H_2O)_3$ isomer A1, and it is also a minimum energy structure on the three-water potential surface, lying about one-half kcal/mol higher in energy than the global minimum A1. The presence of HCl renders the three free hydrogens nonequivalent; thus, as many as eight torsional variants are possible. As indicated above, enumeration of the torsional species is not the main thrust of this study, but the data for A2 should serve to illustrate the variations to be expected among a set of such conformers. In A2 the free hydrogens follow an up/up/down pattern in contrast to the down/up/down of A1. The different orientation causes a small elongation in the H(2)−O(2) H-bond distance because of interhydrogen repulsion. The remaining geometrical parameters (Table 1) and the atomic charges are quite close to the corresponding values in A1.

Isomer B (Figure 3) is completely different from the A structures. It is essentially a cyclic water trimer with HCl resting on top, hydrogen bonded to one of the oxygens. The H−Cl bond is strong, reflected in the calculated bond lengths of 1.315 Å (B3-LYP) and 1.296 Å (MP2). The water trimer moiety is similar to that found experimentally and theoretically to be the most stable structure for isolated water trimer.[37,38,41−43] 6-311+G** B3-LYP and MP2 optimizations of water trimer yield geometries which agree with each other and with previously reported experimental[37,38] and theoretical[41−43] results. The geometric data in Table 1 reveal the slight distortion in the water cluster induced by interaction with HCl.

In structure C (Figure 3) a central double donor, single acceptor water molecule is hydrogen bonded to HCl and the other two waters. B3-LYP and MP2 predictions of the HCl hydrogen bond length and of the H−Cl bond length differ markedly. B3-LYP predicts an HCl separation of 1.364 Å and a hydrogen bond length of 1.571 Å, while MP2 yields, respectively, values of 1.319 Å and 1.666 Å (Table 2). Overall, the B3-LYP geometry is more compact than the MP2. The water−water interactions are weaker than in isomers A and B (see Tables 1 and 2).

The isomer labeled D in Figure 3 is structurally related to C but is more symmetric. The H−Cl separation is longer than in C, 1.389 Å in B3-LYP and 1.332 Å in MP2 calculations. The HCl hydrogen bond to the central waters is 1.499 Å (B3-LYP) and 1.615 Å (MP2), at B3-LYP, the strongest H-bond in this isomer. The charge distribution as reflected in the gross charges is quite similar to that of C. The double donor $(H_2O)_3$ structures of isomers C and D can be compared with similar local minima found by Mó et al.[44] on the $(H_2O)_3$ energy surface. In isomers C and D we find the central water coordinated to three hydrogens, and thus positioned to form hydronium ion were such formation possible.

The remaining structure, E in Figure 3, is one in which HCl is weakly associated with the trimer unit. The calculated HCl bond length of 1.291 Å (B3-LYP, 1.275 Å MP2) shows that HCl is little perturbed by interaction with the waters. The predominant component of bonding appears to be electrostatic attraction between chlorine and the three free hydrogens of the waters.

3.2. $HCl(H_2O)_4$ Clusters. In all three-water clusters HCl remains associated, and in each there is a strong covalent H−Cl bond. In the $HCl(H_2O)_4$ clusters, on the other hand, we find HCl in both associated and in dissociated, ionic, forms.

3.2.1. Associated Structures. The most stable of the associated structures, indeed of all the four-water structures, isomer A (Figure 4) consists essentially of a square water tetramer with HCl sitting on top, hydrogen bonded to one water, and canted slightly from perpendicular. It is reminiscent of structure B of the three-water isomers. The four water molecules are in the configuration, almost unperturbed, of isolated water tetramer in its minimum energy configuration.[38,45,46] Each H_2O of isomer A acts as a hydrogen bond single donor and single acceptor, except that the oxygen to which HCl is attached is a double acceptor. The free hydrogens lie alternately above and below the plane of the square formed by the oxygens. The Cl−H···O hydrogen bond length is 1.797 (DFT), 1.834 Å (MP2). The O−O separation in isolated water tetramer found by MP2/6-311+G** optimization was 2.747 Å, in substantial accord with the MP2/aug-cc-pVDZ distance of 2.785 Å reported by Xantheas and Dunning and with the experimental separations of 2.78−2.79 Å.[42] The O−O distances for the oxygen involved in the H bond with HCl are slightly shortened on one side, lengthened on the other. The gross charges on H (0.28) and Cl (−0.29) reflect a slightly greater charge separation than in isolated HCl. And the acceptor oxygen atom in the HCl H-bond of A is more negative than are the oxygens in $(H_2O)_4$.

Structure B (Figure 4) is a local minimum structure obtained by slightly buckling the four-oxygen square of A. HCl is more nearly parallel to $(H_2O)_4$ permitting some H_2O···Cl interaction. The optimized B3-LYP and MP2 structures differ in the degree of distortion, the B3-LYP structure appearing to be more nearly a cyclic $(H_2O)_3$ cluster hydrogen bonded to the remaining water.

The third isomer is represented by two torsional variants, C1 and C2, in Figure 4. It is a pentagonal, nearly planar structure with chlorine and the four oxygens at the apexes. The hydrogen of HCl is in the middle of a side of the pentagon, hydrogen

TABLE 5: Energies of Low-Lying $HCl(H_2O)_3$ Structures Calculated with 6-311+G Basis Sets**[a]

	B3-LYP		MP2		QCISD(T)	
isomer	energy	Δ energy	energy	Δ energy	energy	Δ energy
A1	−690.2523719	0.00	−689.1121030	0.00	−689.165706	0.00
A2	−690.2514862	0.5558	−689.1113096	0.4979	−689.164946	0.4797
B	−690.2477482	2.9014	−689.1090271	1.9302	−689.163193	1.5800
C	−690.2442539	5.0941	−689.1039627	5.1081	−689.157758	4.9906
D	−690.2446014	4.8761	−689.1044942	4.7746	−689.158377	4.6020
E	−690.2363420	10.0589	−689.0989070	8.2806	−689.153881	7.4230

[a] Isomer labels follow Figure 3. Energies are in atomic units. Δ Energy is the energy in kcal/mol each isomer lies above A1.

bonded to a water. The free hydrogens of the waters lie alternately above and below the plane. Three of the water subunits act as both H-bond donors and acceptors. The final water is a H-bond acceptor and one of its hydrogens interacts weakly with Cl at a distance of 2.3 Å. The HCl bond length of 1.372 Å (B3-LYP, 1.323 Å MP2) is slightly longer than in isomers A and B (Table 3). Again, B3-LYP predicts a longer H−Cl separation and smaller H-bond distances than does MP2.

C1 and C2, which differ in the orientation of two of the free hydrogens, can be viewed as similar to the global minimum cyclic ring structure found for $(H_2O)_5$,[37,42,46] with HCl substituted for a water. Xantheas and Dunning reported a HF/aug-cc-pVDZ optimized planar structure for $(H_2O)_5$ with oxygen−oxygen distances of 2.863, 2.862, 2.863, 2.865, and 2.882 Å. The B3-LYP structure of $HCl(H_2O)_4$ finds O(1)−O(2), O(2)−O(3), O(3)−O(4), Cl−O(4), and Cl−O(5) distances of 2.674, 2.727, 2.746, 3.266, and 2.904 Å, respectively. The corresponding MP2 values are 0.03−0.05 Å longer. The atomic charges of −0.37 for Cl and 0.36 for H show more charge transfer than in A or B, and that is consistent with the slight lengthening of the HCl bond.

3.2.2. Dissociated Structures. The most stable isomer in which HCl is dissociated is labeled D in Figure 5. It is a structure in which three water molecules form the equatorial plane of a trigonal bipyramid, with a Cl^- and an H_3O^+ at the apexes. This structure has been found by Planas and co-workers[17] in B-LYP/TZ94+P calculations; our D agrees well with the structure determined in that study. There are three hydrogens 2.07 Å (B3-LYP) or 2.10 Å (MP2) from Cl, showing a weak interaction. The H_3O^+ shows strong H bonds to the H_2O molecules, with separation distances of about 1.54 Å in DFT calculations and nearly the same in MP2. There are no hydrogen bonds between water molecules. Population analysis demonstrates the ionic character of the structure, with Cl carrying a charge of −0.80, and hydronium ion +0.85.

Finally, two torsional isomers, E1 and E2, are presented in Figure 5. These have elongated HCl separations of 1.70 Å (MP2) or 1.80 Å (B3-LYP). As in structure D, a hydronium ion forms part of the structure. In this case the H_3O^+ hydrogen bonds to two waters, and two waters are hydrogen bonded to each other.

3.3. Energy Ordering and Frequency Analyses. The B3-LYP and MP2 predictions of the order of stability and even the energy differences of the $HCl(H_2O)_3$ clusters agree very well. The QCISD(T)/6-311+G** calculations confirm the order obtained with these methods. Results are presented in Table 5. Isomer A1 is the most stable structure on the potential surface, and its torsional variant, A2, lies less than 0.5 kcal/mol higher at the QCISD(T) level. Structure B lies 2 kcal/mol above A1. All isomers are within 10 kcal/mol in energy of each other and thus are thermally accessible at normal temperatures.

The B3-LYP and MP2 harmonic frequencies for the three-water clusters agree well. The HCl stretch in isomer A1 shows a red-shift of 500 cm^{-1} with respect to isolated HCl. The red-shift accompanies the expected weakening of the bond and is consistent with the observations of Packer and Clary[14] on smaller clusters. The HCl stretching frequency of B is nearly the same as in structure A1. Isomer C shows a very low HCl stretching frequency that correlates with the increase in bond length. The red-shift is reduced in structure D showing the dependence on H−Cl distance. The theoretical frequency synthesis for the most stable isomer, A1, is shown in Figure 6.

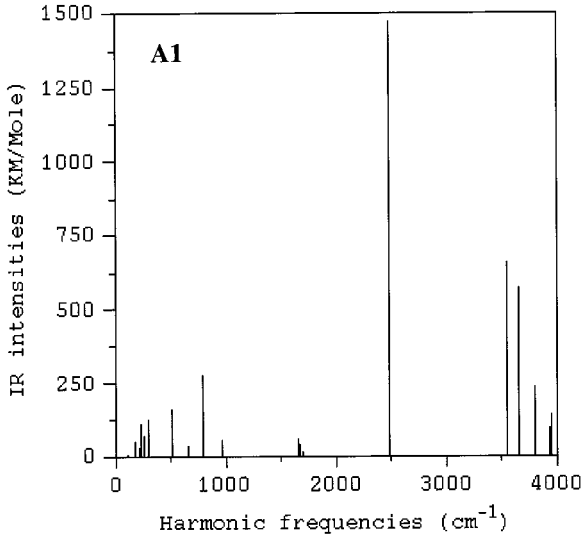

Figure 6. A theoretical construction of the IR (harmonic frequencies) spectrum of $HCl(H_2O)_3$ isomer A1.

For $HCl(H_2O)_4$ clusters, the B3-LYP and MP2 energy orderings do not agree. The results shown in Table 6 indicate that the most stable B3-LYP structure is dissociated isomer D, 1 kcal/mol beneath associated isomer A. MP2, on the other hand, finds A most stable and also finds B to be more stable than D. All-order QCISD(T)/6-311+G* calculations confirm the order found with the MP2 approximation. The calculated harmonic frequencies for isomers A and D are presented in Figure 7. The spectra are seen to be similar enough that distinguishing these species solely on the basis of their IR spectra may well be difficult, a conclusion reached by Delzeit and co-workers[10] in spectroscopic studies of HCl−water clusters. However, the presence of hydronium in the dissociated clusters does produce additional spectral features, one of which at about 3000 cm^{-1} may potentially be useful in identifying this form of the cluster.

4. Conclusions

The MCSA−DFT method has proven to be capable of finding low-lying minima on the potential surfaces of $HCl(H_2O)_3$ and $HCl(H_2O)_4$. As expected, hydrogen bonding was found to play the crucial role in the stability of the HCl clusters, and the several possible H-bond arrangements produced groups of isomers near each other in energy. In each of the three-water clusters, HCl was found to be associated with a strong covalent

TABLE 6: Energies of Low-Lying $HCl(H_2O)_4$ Structures

	B3-LYP[a]		MP2[a]		QCISD(T)[b]	
isomer	energy	Δ energy	energy	Δ energy	energy	Δ energy
A	−766.7277398	0.00	−765.4049391	0.00	−765.3440413	0.00
B	−766.7216942	3.7937	−765.4033126	1.0206	−765.3420040	1.2784
C1	−766.7260878	1.0366	−765.4022916	1.6613	−765.3401756	2.4258
C2	−766.7261931	0.9706	−765.4021909	1.7245	−765.3398411	2.6357
D	−766.7293318	−0.9990	−765.4014781	2.1718	−765.3418012	1.4057
E1	−766.7266016	0.7142	−765.3993221	3.5247	−765.3383718	3.5577
E2	−766.7252820	1.5423	−765.3990025	3.7253	−765.3380152	3.7814

[a] Energies calculated with 6-311+G** basis sets. [b] Energies calculated with 6-311+G* basis sets. Isomers are indicated by the labels they take in Figures 4 and 5. Energies are in atomic units. Δ Energy refers to the energy (kcal/mol) above isomer A.

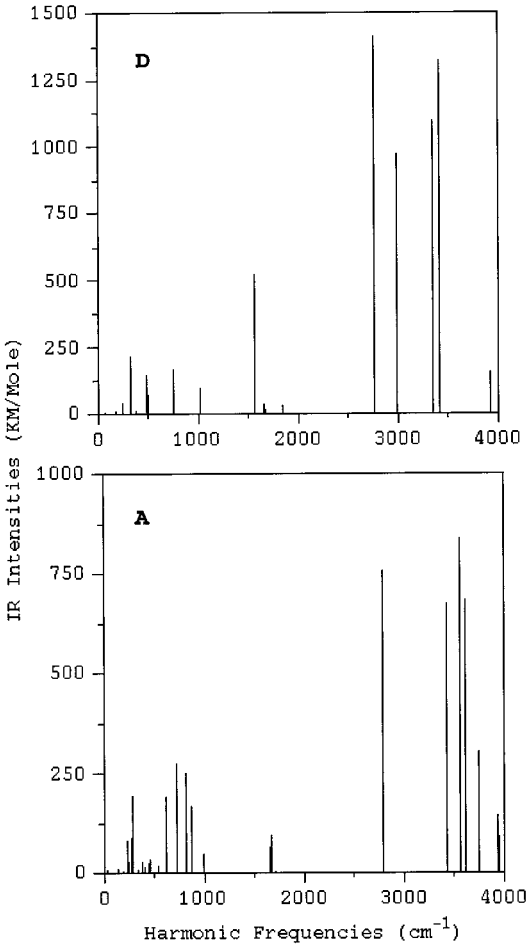

Figure 7. Predicted IR spectra of $HCl(H_2O)_4$ isomers A(below) and D (above). Although in A HCl remains associated, while in D it is ionized, the spectra have many features in common.

H−Cl bond. Clearly in isomers C and D (Figure 3) we see configurations in which the oxygen of one water molecule is coordinated to three hydrogens, one of them from H−Cl. These indicate an incipient hydronium ion formation, but it appears that one more water is needed to stabilize Cl^- before H_3O^+ can form fully. In $HCl(H_2O)_4$, on the other hand, HCl in both its ionized and associated states is to be found in clusters separated by small energy differences. The global minimum structure for $HCl(H_2O)_4$ is one in which HCl is bound, but the lowest-energy dissociated structure lies only 1.4 kcal/mol in energy above it at the QCISD(T) level. It therefore seems that the 3- to 4-water transition marks a threshold beyond which a sufficient number of solvent molecules exists to stabilize the hydronium and chloride ions created by dissociation of HCl.

All of the isomers show an anticorrelation between intermolecular H-bond length (O···H) and the intramolecular O−H distance; as a hydrogen bond shortens, the intramolecular O−H bond to the same hydrogen lengthens. The behavior is noted at both of the theoretical levels employed in this study and has been observed in water tetramer and in crystal structures of chemically related H-bonded molecules.[36] For the free hydrogens, the O−H bond length remains constant to within 0.001 Å at both levels of theory for all isomers. As expected, the variations in energy among torsional conformers was found to be somewhat smaller than those noted overall among the structural isomers.

We find in general that the structural complexity of the HCl−water potential surface is well described by both the B3-LYP and the MP2 theoretical models with 6-311+G** basis sets. The optimized geometrical parameters displayed in Tables 1−4 exhibit two clear overall differences between the two theoretical levels employed. The HCl bond length is overestimated in the B3-LYP calculations when compared to the MP2, and all structures show an underestimation of H-bond interactions by B3-LYP as compared to MP2.

Acknowledgment. This work has been supported by NSF and NASA through the EPSCoR program. The authors are grateful for computer time provided by the RCMI Center for Molecular Modeling and Computational Chemistry.

References and Notes

(1) McElroy, M. B.; Salawitch, R. J. *Science* **1989**, *243*, 763.
(2) Solomon, S. *Nature* **1990**, *347*, 347.
(3) Brune, W. H.; Anderson, J. G.; Toohey, D. W.; Fahey, D. W.; Kawa, S. R.; Jones, R. L.; McKenna, D. S.; Poole, L. R. *Science* **1991**, *252*, 1260.
(4) Beig, G.; Walters, S.; Brasseur, G. J. *J. Geophys. Res.* **1993**, *98*, 775.
(5) Webster, C. R.; May, R. D.; Toohey, D. W.; Avallone, L. M.; Anderson, J. G.; Newman, P.; Lait, L.; Schoeberl, M. R.; Elkins, J. W.; Chan, K. R. *Science* **1993**, *261*, 1130.
(6) Rowland, F. S. *Ann. Rev. Phys. Chem.* **1991**, *42*, 731.
(7) Sodeau, J. R.; Horn, A. B.; Banham, S. F.; Koch, T. G. *J. Phys. Chem.* **1995**, *99*, 6258.
(8) Molina, L. T.; Molina, M. J.; Stachnik, R. A.; Tom, R. D. *J. Phys. Chem.* **1985**, *89*, 3779.
(9) Angel, L.; Stace, A. J. *J. Chem. Soc., Faraday Trans.* **1997**, *93*, 2769.
(10) Delzeit, L.; Rowland, B.; Devlin, J. P. *J. Phys. Chem.* **1993**, *97*, 10312.
(11) Kroes, G. J.; Clary, D. C. *J. Phys. Chem.* **1992**, *96*, 7079.
(12) Robertson, S. H.; Clary, D. C. *Faraday Discuss.* **1995**, *100*, 309.
(13) Gertner, B. J.; Hynes, J. T. *Science* **1996**, *271*, 1563.
(14) Packer, M. J.; Clary, D. C. *J. Phys. Chem.* **1995**, *99*, 14323.
(15) Møller, C.; Plesset, M. S. *Phys. Rev.* **1934**, *46*, 618.
(16) Amirand, C.; Maillard, D. *J. Mol. Struct.* **1988**, *176*, 181.
(17) Planas, M.; Lee, C.; Novoa, J. J. *J. Phys. Chem.* **1996**, *100*, 16495.
(18) Geiger, F. M.; Hicks, J. M.; de Dios, A. C. *J. Phys. Chem.* **1998**, *102*, 2A, 1514.
(19) Ando, K.; Hynes, J. T. *J. Phys. Chem.* **1997**, *101*, 1B, 10464.
(20) Kirkpatrick, S.; Gellat, C. D., Jr.; Vecchi, M. P. *Science* **1983**, *220*, 671.
(21) Metropolis, N.; Rosenbluth, A. W.; Rosenbluth, M. N.; Teller, A. H.; Teller, E. *J. Chem. Phys.* **1953**, *21*, 1087.

(22) Okamoto, Y.; Kikuchi, T.; Kawai, H. *Chem. Lett.* **1992**, 1275. Wilson, S. R.; Cui, W.; Moskowitz, J. W.; Schmidt, K. E. *Tetrahedron Lett.* **1988**, *29*, 4373.
(23) Keshari, V.; Ishikawa, Y. *Chem. Phys. Lett.* **1994**, *218*, 406. Keshari, V.; Ishikawa, Y. *Int. J. Quantum Chem. Symp.* **1994**, *28*, 541.
(24) Ishikawa, Y.; Binning, R. C., Jr.; Sekino, H. *Int. J. Quantum Chem. Symp.* **1995**, *29*, 669.
(25) Becke, A. D. *J. Chem. Phys.* **1988**, *88*, 1053.
(26) Lee, C.; Yang, W.; Parr, R. G. *Phys. Rev.* **1988**, *B37*, 785.
(27) Hehre, W. J.; Ditchfield, R.; Pople, J. A. *J. Chem. Phys.* **1972**, *56*, 2257.
(28) Pople, J. A.; Schlegel, H. B.; Krishnan, R.; DeFrees, D. J.; Binkley, J. S.; Frisch, M. J.; Whitesides, R. A.; Hout R. J.; Hehre, W. J. *Int. J. Quantum Chem. Symp.* **1981**, *15*, 269.
(29) Curtiss, L. A.; Raghavachari, K. *Quantum Mechanical Electronic Structure Calculations with Chemical Accuracy*; Langhoff, S., Ed.; Kluwer: Dordrecht, 1994.
(30) Ziegler, T. *Chem. Rev.* **1991**, *91*, 651.
(31) Mlynarski, P.; Salahub, D. R. *J. Chem. Phys.* **1991**, *95*, 6050.
(32) Bacelo, D. E.; Ishikawa, Y. *J. Mol. Struct. (THEOCHEM)* **1998**, *425*, 87.
(33) Kim, K.; Jordan, K. D. *J. Phys. Chem.* **1994**, *98*, 10089. Novoa, J. J.; Sosa, C. *J. Phys. Chem.* **1995**, *99*, 15837.
(34) Gaussian 94, Revision E.1: Frisch, M. J.; Trucks, G. W.; Schlegel, H. B.; Gill, P. M. W.; Johnson, B. G.; Robb, M. A.; Cheeseman, J. R.; Keith, T. A.; Petersson, G. A.; Montgomery, J. A.; Raghavachari, K.; Al-Laham, M. A.; Zakrzewski, V. G.; Ortiz, J. V.; Foresman, J. B.; Cioslowski, J.; Stefanov, B. B.; Nanayakkara, A.; Challacombe, M.; Peng, C. Y.; Ayala, P. Y.; Chen, W.; Wong, M. W.; Andres, J. L.; Replogle, E. S.; Gomperts, R.; Martin, R. L.; Fox, D. J.; Binkley, J. S.; Defrees, D. J.; Baker, J.; Stewart, J. P.; Head-Gordon, M.; Gonzalez, C.; Pople, J. A.; Gaussian, Inc.: Pittsburgh, PA, 1995.
(35) Pople, J. A.; Head-Gordon, M.; Raghavachari, K. *J. Chem. Phys* **1987**, *87*, 5968.
(36) Schütz, M.; Klopper, W.; Lüthi, H. P.; Leutwyler, S. *J. Chem. Phys.* **1995**, *103*, 6114.
(37) Liu, K.; Cruzan, J. D.; Saykally, R. J. *Science* **1996**, *271*, 929.
(38) Liu, K.; Loeser, J. G.; Elrod, M. J.; Host, B. C.; Rzepiela, J. A.; Pugliano, N.; Saykally, R. J. *J. Am. Chem. Soc.* **1994**, *116*, 3507.
(39) Re, S.; Osamura, Y.; Suzuki, Y.; Schaefer, H. F. *J. Chem. Phys.* **1998**, *109*, 977.
(40) Smith, A.; Vincent, M. A.; Hillier, I. H. *J. Phys. Chem. A* **1999**, *103*, 1132.
(41) Kim, K. S.; Dupuis, M.; Lie, G. C.; Clementi, E. *Chem. Phys. Lett.* **1986**, *131*, 451.
(42) Xantheas, S. S.; Dunning, T. H. *J. Chem. Phys.* **1993**, *99*, 8774.
(43) Estrin, D. A.; Paglieri, L.; Corongiu, G.; Clementi, E. *J. Phys. Chem.* **1996**, *100*, 8701.
(44) Mó, O.; Yánez, M.; Elguero, J. *J. Chem. Phys.* **1992**, *97*, 6628.
(45) Cruzan, J. D.; Braly, L. B.; Liu, K.; Brown, M. G.; Loeser, J. G.; Saykally, R. J. *Science* **1996**, *271*, 59.
(46) Xantheas, S. S. *J. Chem. Phys.* **1994**, *100*, 7523.